Chapter 4

NEW NONLINEAR OPTICAL EFFECTS IN NEMATICS AND CHOLESTERICS DUE TO DIRECTOR REORIENTATION

A pure Thought-Mind surveyed the cosmic act.

Sri Aurobindo in Savitri. -p 259

4.1 Introduction

Nonlinear optics in liquid crystals due to the director reorientation in a laser beam has been an important topic of research. It so happens that this process as said earlier leads to giant optical nonlinearities which is $10^6 - 10^8$ times that found in liquids like CS_2 [1, 2, 3]. Incidentally, the nonlinear coefficient in liquid crystals is very sensitive to the initial director orientation and sample preparation [4. 5]. Nematic liquid crystals have been explored in great detail. Yet, cholesterics has nor drawn as much attention in the study of nonlinear optical effects permitted in them. Amongst the first few studies in these liquid crystals mention may be made of H. G. Winful's investigations. He reported optical bistability in these systems [6]. Only a year earlier to this Ye and Shen studied the optical field induced helical structures near the isotropic-cholesteric transition [7]. After the first obsenation of giant optical nonlinearities in nematics, Zeldovich and his collaborators worked out the theory of the orientational nonlinearity in the cholesterics [8, 9]. Lee et. al., studied the

cholesterics in the Bragg geometry and observed the self-focusing of the reflected beam which was explained again on the basis of director reorientation process [10]. Zeldovich and his group have extensively studied the process of director reorientation in cholesterics apart from other liquid crystals and a few of the nonlinear optical effects is summarised in their review article [4]. Here we study the effect of the optical field in a nematic, ferronematic and a cholesteric in the presence of an external static magnetic and electric fields. In situations where the director reorientation is absent we look at the implications of the usual classical Kerr nonlinearity.

4.2 Nematic in a Standing Wave

We now consider a case where a uniform nematic is in a tilted configuration as shown in the figure 4.1 (a). A laser beam linearly polarized in the plane of director tilt is incident normal to the sample surface. Due to the reflection at the other boundary we get a standing wave inside the medium. The electric field of the standing wave results in a reorienting torque on the director. Since in the standing wave the electric field is periodic inside the medium we expect a periodic variation in the director tilt also. The director torque is maximum in the regions of the highest field strengths i.e., at the antinodes. As in the previous cases in a standing wave described in chapter 2 here also we get a reflection of the incident laser beam. To start with, at low intensities only a weak reflection off the bounding rear surface contributes to the field of the standing wave. At these intensities the standing wave field at the antinodes is not strong enough to reorient the uniformly tilted director. As the laser intensity increases the reflected component also increases which in turn increases the amplitude at the antinodes. The ensuing increase in the torque on the director may lead to an appreciable change in the director configuration leading to a periodic variation in the director tilt as shown schematically in the figure 4.1 (b). This periodic structure Bragg reflects all the more the incident light.

In short we again find a total reflection of the incident light or *self – iridescence*. We must remark here that the same effect could be expected in princi-

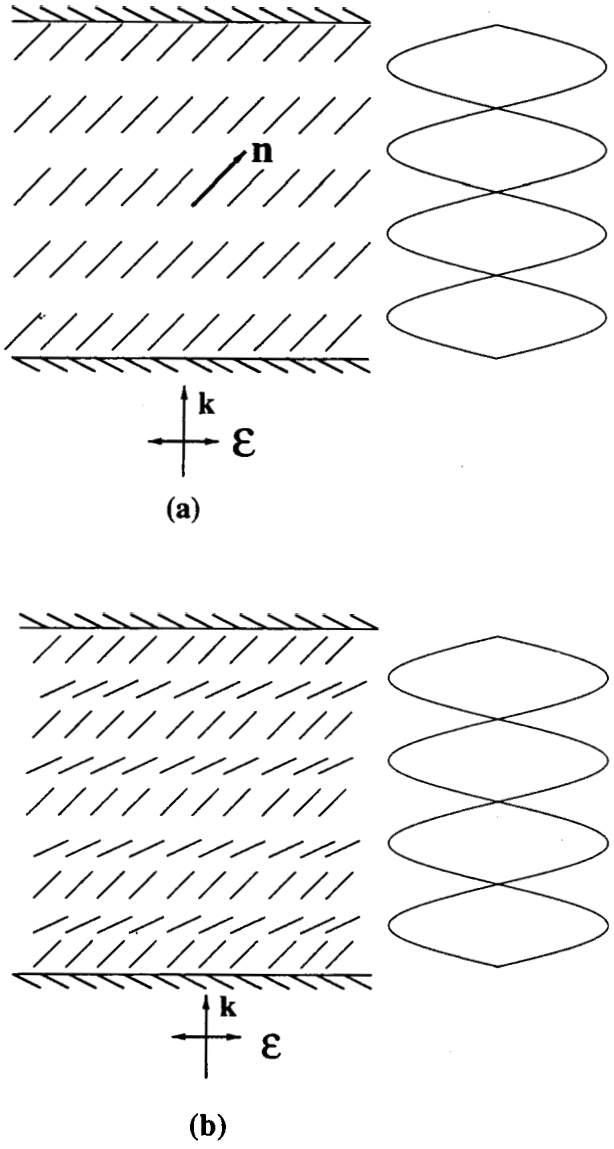

Figure 4.1: *(a) A tilted nematic. The director is anchored at the boundaries at an angle to the glass plates. The polarization of the laser field is parallel to the plates in the plane of the tilt. The nodes and antinodes of the standing wave at very low intensities have also been shown. (b) The periodic variation of the director tilt due to reorientation induced by the standing wave set up in the medium.*

ple even in other materials like the usual crystals. But in view of the smallness of the Kerr coefficient in such media the effect may not be strong enough to lead to self-iridescence.

4.3 Nematic in Magnetic and Optical Fields

Now we consider the contribution to the free energy density by electric and magnetic fields of a laser beam. Even though these fields oscillate at a high frequency of $10^{14} - 10^{15} Hz$ they can exert a torque on $\mathbf{n}$ since the torque arising from dielectric and diamagnetic anisotropy of the medium depends quadratically on the field. In principle there is a contribution to the free energy density from both electric and magnetic fields. In fact, the two energy densities are equal in vacuum. But, in nematics both the diamagnetic susceptibility and its anisotropy are very small each being of the order of 10^{-6}. Hence for optical fields $\epsilon|\mathcal{E}|^2 = |\mathcal{H}|^2$, where ϵ is the dielectric constant, E and $\mathcal{H}$ are electric and magnetic fields of the laser beam. In an anisotropic medium the free energy density due to the optical field is given by [4, 11]:

$$\mathcal{F}_o = -\sum_{j,k} \frac{\epsilon_{jk}}{8\pi} \mathcal{E}_j(\mathbf{r},t)\mathcal{E}_k(\mathbf{r},t) \qquad j,k = x,y,z \tag{4.1}$$

where, ϵ_{jk} is the second rank dielectric tensor of the medium, $\mathcal{E}_j(\mathbf{r},t)$ is a component of the electric field of the light wave. We have to solve the Maxwell wave equation for the laser wave in the medium. That is, E must be obtained from :

$$\nabla \times (\nabla \times \mathcal{E}(\mathbf{r})) - \frac{\omega^2}{c^2}\mathcal{D}(\mathbf{r}) = 0 \tag{4.2}$$

w is the frequency of the light wave, c is the velocity of light and $\mathcal{D}$ is the displacement vector whose components are given by $\mathcal{D}_j = \sum_k \epsilon_{jk}\mathcal{E}_k$. The determination of the steady state structure requires a knowledge of E permitted by the Maxwell equations.

The eigenstates of the electric field vector E, which go through the medium unaltered, are $\mathcal{E}$ parallel and perpendicular to the director n. In this chapter, we consider cases when the director is confined to $x - z$ plane. Also we restrict ourselves to a linearly polarised light wave propagating along z-axis with its electric vector E

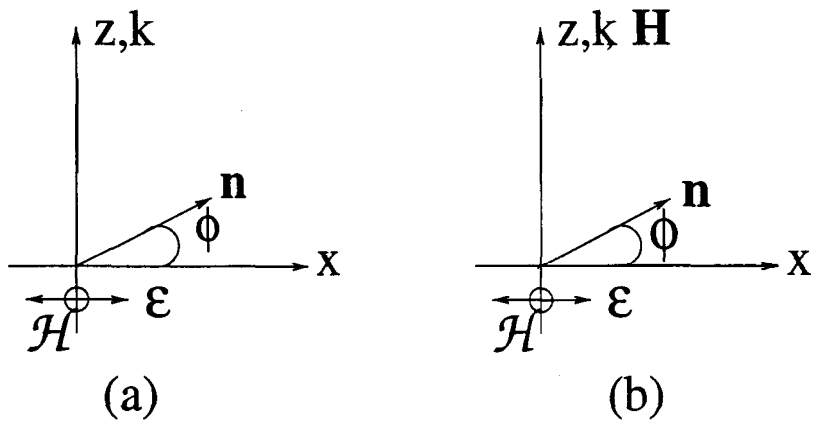

Figure *4.2: Geometries showing the orientation of the director* n *with respect to the electric field* $\mathcal{E}$ *of the incident light and a static magnetic field* H. *(a)* $H = 0$; *(b) H* is *perpendicular to* $\mathcal{E}$, *k is the direction of propagation of the light,* $\mathcal{H}$ is *the magnetic vector associated with the light which is perpendicular to the plane of the figure.*

along x-axis. Then field $\mathcal{E}$ variations are also along z. The geometry is depicted in figure *4.2* (a). It is easy to see from the geometry that the polarisation of the light wave is preserved during its passage through the medium. The Maxwell wave equation is solved in the approximation that the director distortions in the medium are on a length scale large compared to the wavelength of light. Then solutions to the wave equation *(4.2)* become [4]:

$$\mathcal{E}_x(z) = A(\epsilon_\perp + \epsilon_a \sin^2\phi)^{\frac{1}{4}} \times exp[-i\, k_o(\epsilon_\parallel\, \epsilon_\perp)^{\frac{1}{2}} \int^z (\epsilon_\perp + \epsilon_a \sin^2\phi)^{-\frac{1}{2}} dz'] \qquad (4.3)$$

$$\mathcal{E}_z(z) = -A\frac{\epsilon_a \sin\phi \cos\phi}{(\epsilon_\perp + \epsilon_a \sin^2\phi)^{\frac{3}{4}}} \times exp[-i\, k_o(\epsilon_\parallel\, \epsilon_\perp)^{\frac{1}{2}} \int^z (\epsilon_\perp + \epsilon_a \sin^2\phi)^{-\frac{1}{2}} dz'] \qquad (4.4)$$

where, $k_o = \omega/c$, A is the amplitude of the light wave and $\phi \equiv \phi(z)$ is the angle between the director n and the electric vector $\mathcal{E}$. Then from equations (4.1), *(4.3)* and *(4.4)* the optical field free energy density becomes:

$$\mathcal{F}_{optical} = -I\frac{(\epsilon_\parallel\epsilon_\perp)^{\frac{1}{2}}}{(\epsilon_\perp + \epsilon_a \sin^2\phi)^{\frac{1}{2}}} \qquad (4.5)$$

where $I(= \frac{|A|^2}{8\pi c}(\epsilon_\parallel\epsilon_\perp)^{\frac{1}{2}})$ is a measure of the intensity of light. We note that in the limit of small dielectric anisotropy $\mathcal{F}_o$ goes over to the familiar expression for the field contribution to free energy density in static electric fields, viz., $F_{elec} = -\epsilon_a E^2 \cos^2\phi$.

It is important to point out the salient features peculiar to the nonlinear optical reorientation effects as compared to reorientational effects in static electric

fields. In the optical case, the Maxwell equation $\nabla \cdot \mathcal{D} = 0$ leads in the plane wave approximation to $\mathbf{k} \cdot \mathcal{D} = 0$, where $\mathbf{k}$ is the direction of light propagation. This implies that the component $\mathcal{D}_z$ vanishes identically. Since $\mathcal{D}_z = \sum_i \epsilon_{zi} \mathcal{E}_i$ and $\mathcal{E}_y = 0$ we get $\mathcal{E}_z = \epsilon_{zx}/\epsilon_{zz}\, \mathcal{E}_x$. The equation (4.4) has been obtained from equation (4.3) using this relation. On the other hand, in the case of the static field we have the two Maxwell equations *viz.*, V x E = 0 and V . D = 0. The first of these equations leads to the relation $\frac{\partial E_x}{\partial z} = 0$ and hence E_x is a constant. The second equation with appropriate boundary conditions again implies $D_z = 0$ thus leading to the same relation between E_x and E,. Hence instead of equations (4.3) and (4.4) we get in the case of static fields E_x = constant and $E_z = \epsilon_a \sin\phi \cos\phi\, E_x/(\epsilon_\perp + \epsilon_a \sin^2\phi)$.

The magnetic free energy density of a nematic in a static magnetic field is given by:

$$F_{mag} = -\frac{\chi_\perp}{2} \mathbf{H}^2 - \frac{\chi_a}{2} (\mathbf{n} \cdot \mathbf{H})^2 \tag{4.6}$$

where $\mathbf{n}$ is the nematic director, H is the static magnetic field, χ_a is the diamagnetic anisotropy which is equal to $(\chi_\parallel - \chi_\perp)$ with $\chi_\parallel$ and $\chi_\perp$ as respectively the diamagnetic susceptibilities parallel and perpendicular to the director. In a free sample $\mathbf{n}$ will be either parallel or perpendicular to the magnetic field depending on whether χ_a is positive or negative.

We now consider 'the effect of the electric field $\mathcal{E}$ of the light wave on a nematic in the presence of an external magnetic field. Then the net field free energy density is $\mathfrak{Z} = \mathcal{F}_m + \mathcal{F}_o$. The different geometries which could be studied include the electric field of the light wave $\mathcal{E}$ being either parallel or perpendicular to the static magnetic field H with ϵ_a and χ_a being positive or negative.

We discuss only one geometry shown in figure 4.2 (b) where $\mathcal{E}$ is perpendicular to H and both ϵ_a and χ_a are positive. The corresponding equation of equilibrium obtained by minimising the total free energy is:

$$\frac{\mathbf{I}\, \epsilon_\parallel^{\frac{1}{2}}\, \tau \sin\phi \cos\phi}{(1 + \tau \sin^2\phi)^{\frac{3}{2}}} - \chi_a H^2 \sin\phi \cos\phi = 0 \tag{4.7}$$

where $\tau = \epsilon_a/\epsilon_\perp$. It is clear from equation (4.7) that the torque acting on the director

due to the static magnetic field H opposes that due to the electric field $\mathcal{E}$ of the light wave.

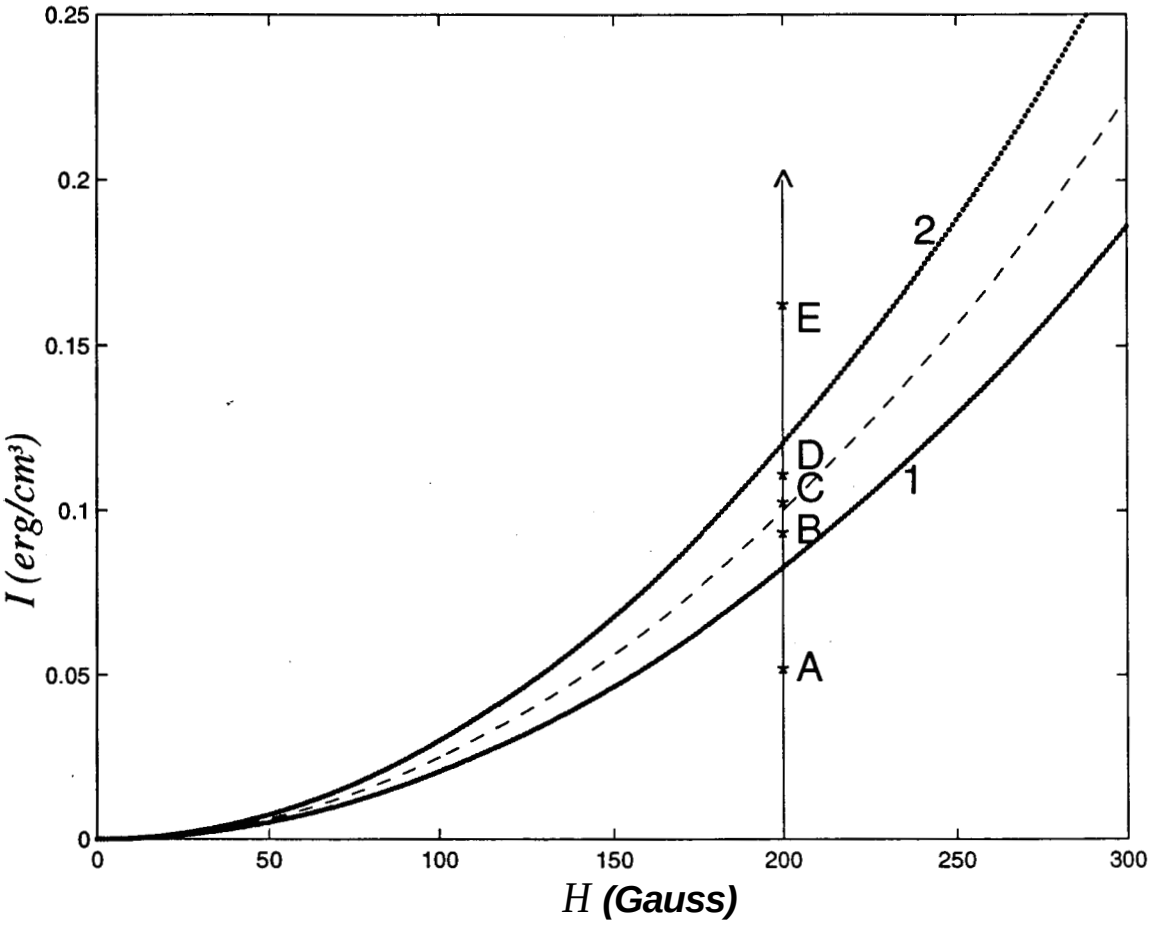

Figure 4.3: *Phase diagram for the uniform state in a nematic. The dashed curve is a line of first order transition. The dotted lines 1 and 2 are stability lines. Here I is the measure of intensity.* $\epsilon_{||} = 2.89$, $\epsilon_{\perp} = 2.25$, $K = 10^{-6}$ *dyne.*

We have worked out the different uniform states permitted by equation (4.7). In the uniform state the director $\mathbf{n}$ can be either parallel$(\phi = 0)$ or perpendicular$(\phi = \pi/2)$ to the electric field $\mathbf{I}$. The allowed uniform states are obtained by appealing to the total free-energy. There can be a switch over from one uniform state to the other as either $\mathbf{I}$ or H is changed. The phase diagram so obtained is as shown in figure 4.3. We also find metastable states in the system. These are states with minima in the total free-energy functional but not the global minima. The dashed line in the phase diagram is a line of coexistence of the two states with $\phi = 0$ and $\frac{\pi}{2}$. The dotted lines 1 and 2 are lines of stability across which a particular orientation of the director goes from an unstable state to a metastable state and *viceversa.* The orientation of the

director in the different regions A, B, C, D, and E are given in Table 4.1.

Table 4.1: *The orientations of the Uniform states in the different regions of the phase diagram shown in figure* 4.3

	Uniform State		
Region	Stable States		Metastable States
A	$-\pi/2$	$\pi/2$	-
B	$-\pi/2$	$\pi/2$	0
C	$\pi/2$	0	-
D	0	π	$\pi/2$
E	0	π	-

4.3.1 Ferronematics in magnetic and optical fields

Ferronematics are a dilute uniform suspension of needle like magnetic grains in a nematic. The grains preferentially get aligned along the local nematic director when the system is cooled from its isotropic phase in an external magnetic field. The director orientation in these systems may be altered by the application of static magnetic fields as low as 10-100 Gauss. On the other hand, to effect the same change in a normal nematic, magnetic fields as high as $1\ kG$ would be required because of the small value of the diamagnetic anisotropy. Further, if the grain concentration is low enough, it will not alter the passage of light through the medium. In a ferronematic there are additional contributions to the free energy density, one due to ferromagnetic interaction with the external field and the other due to entropy of mixing between the guest(magnetic grains) and host(nematic). The net contribution first worked out be de Gennes et. al., is given by [12]:

$$\mathcal{F}_{fn} = -\mathbf{M}.\mathbf{H} + \frac{f\ k_B\ T\ \ln f}{\Omega} \tag{4.8}$$

Here f is the volume fraction of ferromagnetic grains in the nematic matrix, M is the magnetisation in the medium, k_B is Boltzmann's constant, T is the absolute temperature and Ω is the volume of the sample. Due to mechanical coupling between the grains and the director $\mathbf{n}$, the average magnetisation M is along $\mathbf{n}$ and the

magnitude of M is f times the average grain magnetisation. In these systems. the uniform state has a constant f.

Due to an increase in the number of independent parameters in ferronemarics, we have many more possibilities. Here M can be either parallel or antiparallel to H with ϵ_a and χ_a being positive or negative. For the purposes of our dixussion here we treat only the following two cases since these exhibit some new and interesting features.

CaseI : E perpendicular to $\mathbf{H}, \epsilon_a > 0, \chi_a < 0$ and M parallel to H

Case11 : *E* perpendicular to $\mathbf{H}, \epsilon_a > 0, \chi_a > 0$ and M parallel to H

The other cases are similar to one or the other of these two cases. We discuss the first case in detail.

Case *I*

The geometry for this case is depicted in figure 4.2 (b). The free energy density of a ferronematic in a static magnetic field in the presence of a laser field is obtained by adding equations (4.5), (4.6) and (4.8) i.e.,

$$\mathcal{F} = -\frac{I\,\epsilon_{\|}^{\frac{1}{2}}}{(1 + \tau \sin^2\phi)^{\frac{1}{2}}} + \frac{|\chi_a|}{2} H^2 \sin^2 o - m f H \sin\phi + \frac{f k_B T \ln f}{\Omega} \tag{4.9}$$

where m is the average magnetisation of an individual grain.

In the uniform state of a ferronematic there is no grain segregation and therefore f is a constant. Hence the last term in the free energy is a constant. The uniform states are obtained by minimising equation (4.9):

$$\frac{I\,\epsilon_{\|}^{\frac{1}{2}}\,\tau \sin\phi \cos\phi}{(1 + \tau \sin^2\phi)^{\frac{3}{2}}} + |\chi_a|\, H^2 \sin\phi \cos\phi - m f H \cos o = 0 \tag{4.10}$$

The permitted uniform states are (i) n along the magnetic field($o = \pi/2$) and (ii) n at an angle to the field($\phi = \phi_o$). The phase diagram for the transition between these permitted uniform states is depicted in figure 4.4. The transition from one uniform state to another in this case is of second order. In the region A we have $o = \pi/2$ and in the region B, $\phi = \phi_o$. One interesting feature of this case should be stressed here.

At a constant optical intensity below a threshold value, when the magnetic field is

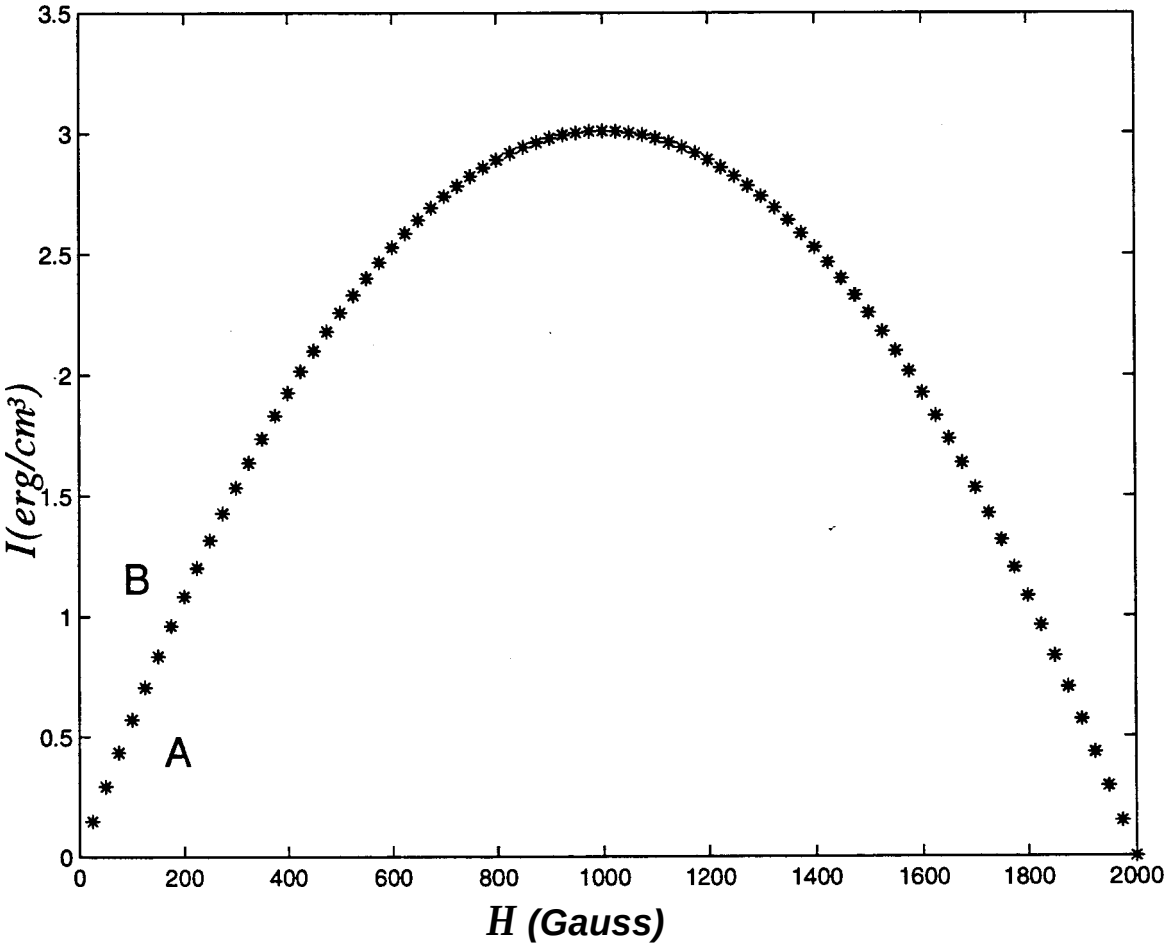

Figure **4.4:** *Phase diagram for the uniform state of a ferronematic with $\mathcal{E}$ perpendicular to H, $\epsilon_a > 0$, $\chi_a < 0$, M parallel to H. The starred curve is a line of second order transition. In all our calculations in a ferronematic we have used the parameters m = 2 Gauss, $\rho = \frac{m\Omega}{k_B T}$ = 0.02 Gauss^{-1}, $\bar{f} = 10^{-3}$ and $\chi_a = 10^{-6}$ cgs.*

continuously increased the system undergoes a transition from a uniform state with $\phi = \phi_\circ$ to another uniform state with $\phi = \pi/2$ and returns back to the initial uniform state *i.e.*, $\phi = \phi_\circ$. Thus the system exhibits a reentrant phenomenon. Table **4.2** gives the orientations found in different regions.

Table **4.2:** *The various orientations of the Uniform state in the different regions of the phase diagram shown in figure* **4.4**

	Uniform State			
Region	*Stable States*		*Metastable States*	
A	$\pi/2$	$5\pi/2$	-	-
B	$\pi/2$	$5\pi/2$	$\phi_\circ$	$3\pi - \phi_\circ$

Case II

The geometry in this case is again the same i.e., the one shown in figure **4.2** (b). The permitted uniform states are (i) **n** along the magnetic field($\$ = \pi/2$) and **(ii) n** at an angle to the field($\$ = \phi_o$). The phase diagram for the transition between these

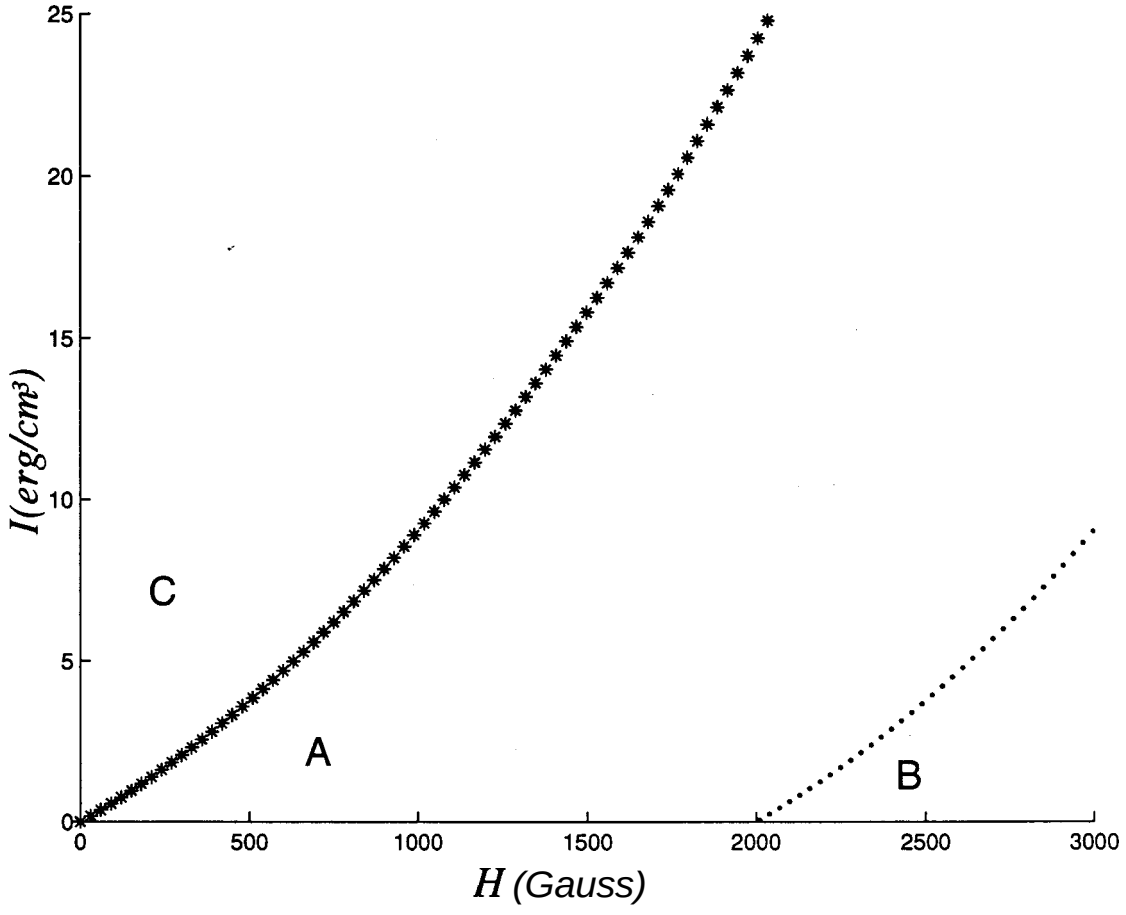

Figure **4.5:** *Phase diagram for the uniform state of a ferronematic with $\mathcal{E}$ perpendicular to H, $\epsilon_a > 0$, $\chi_a > 0$ and* M *parallel to H. The starred line represents a second order transition. Dotted line* is *a line of stability.*

permitted uniform states is depicted in figure **4.5.** The transition from one uniform state to another in this case is of second order. In the region **A** we have the stable state at $\phi = \pi/2$ and in the region C, $\phi = \phi_o$. In region B, the stable states are same as in region **A** and in addition we also have $\phi = 3\pi/2$ which is metastable. The starred line in figure **4.5** is a line of second order phase transition and the dotted line is a line of stability. Interestingly, reentrant behaviour is not seen in this case. Table **4.3** gives the orientation of the director in the different regions of the phase diagram.

Table *4.3: The various orientations of the Uniform state in the different regions of the phase diagram in figure 4.5*

	Uniform State				
Region	*Stable States*		*Metastable States*		
A	$\pi/2$	$5\pi/2$	-	-	-
B	$\pi/2$	$5\pi/2$	-	$3\pi/2$	-
C	$\pi - \phi_o$	ϕ_o	-	-	-

4.4 Cholesterics

We next study the new nonlinear optical defects due to director reorientation process in cholesterics.

4.4.1 Global structural switching:

We have mentioned in the introduction that [13], in the Mauguin limit, the eigenmodes are linearly polarized waves. The electric vector is either parallel or perpendicular to the local nematic director everywhere. Consider the system in a configuration where one beam, say beam *1* has its electric vector parallel to the local director and the other, say beam *2* perpendicular to the director. The beams are in general of different wavelengths.

Figure *4.6* illustrates this situation when the beams are counter-propagating. The corresponding free-energy density obtained by generalising that for a single beam is given by:

$$\mathcal{F} = -\epsilon_a(1)\, I_1/16\pi c + \epsilon_a(2)\, I_2/16\pi c \qquad (4.11)$$

Here I_1 and I_2 are the intensities of the two beams and c is the velocity of light. The positive dielectric anisotropies $\epsilon_a(1)$ and $\epsilon_a(2)$ are defined by $\epsilon_a(i) = \epsilon_{\parallel}(i) - \epsilon_{\perp}(i); i = 1, 2$, where $\epsilon_{\parallel}(i)$ and $\epsilon_{\perp}(i)$ are the dielectric constants parallel and perpendicular to the director. They could be different for the two beams due to the

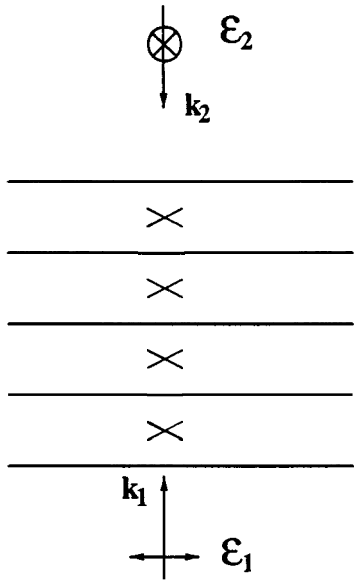

Figure 4.6: *Two counter-propagating beams in a cholesteric liquid crystal in the Mauguin limit. The wave vectors of the two beams are parallel to the twist axis. The electric vector of beam 1* is *parallel to the local director and that of beam 2* is *perpendicular to the local director.*

natural optical dispersion in the medium. To start with let $I_1\epsilon_a\,(1) \gg I_2\epsilon_a\,(2)$ then $\mathcal{F} < 0$ and the system will adopt a configuration where locally the director is along the electric field of beam *1*. When the intensity of beam *2* is increased with respect to beam *1*, the free-energy density becomes positive ($\mathcal{F} > 0$) above a threshold intensity given by:

$$I_{2th} = \epsilon_a(1)\; I_1/\epsilon_a(2) \tag{4.12}$$

In order to reduce the energy, the cholesteric will globally *switch* to a configuration such that the electric field of the beam **2** is everywhere parallel to the director. In this state the free-energy density again becomes negative.

If the two dielectric anisotropies $\epsilon_a(1)$ and $\epsilon_a(2)$ are negative then beam **1** whose electric vector is parallel to the director is not in a favorable state but beam 2 is in a favorable state. If now the intensity of beam *1* is increased with respect to beam *2* then as in the previous case, beyond a threshold intensity, the cholesteric will rotate globally through $\pi/2$ to minimize the total free-energy.

Bibliography

[1] I. C. Khoo and S. T. Wu. *Optics and Non-linear Optics of Liquid Crystals*, (World Scientific, Singapore) 1993

[2] I. C. Khoo, *Liquid Crystals, Physical Properties and Nonlinear Optical Phenomena* (John Wiley and sons, New York) 1995

[3] F. Simoni, *Nonlinear Optical Properties of Liquid Crystals and Polymer Dispersed Liquid Crystals.,* (World Scientific, Singapore) 1997

[4] N. V. Tabiryan, A. V. Sukhov and B. Ya. Zel'dovich, Mol. Cryst. Liq. Cryst., 136, 1 (1986)

[5] Simoni. F, Liq. Cryst., **24(1)**, 83 (1998)

[6] H. G. Winful, Phy. Rev. Lett., 49, 1179 (1982)

[7] P. Ye and Y. R. Shen, App. Phy., 25, 49 (1981)

[8] B. Ya. Zeldovich et. al., Mol. Cryst. Liq. Cryst., 69, 12 (1980)

[9] B. Ya. Zeldovich et. al., Sov. Phy. JETP, 55, 99 (1982)

[10] J. C. Lee et. al., Mol. Cryst. Liq. Cryst., **150B**, 617 (1987)

[11] H. L. Ong, Phys. Rev., **A28**, 2933 (1982)

[12] F. Brochard and P. G. de Gennes, J Phys. France 31,$91 (1970)

[13] S. Chandrashekar, *Liquid Crystals* (second edition), Cambridge University Press, Cambridge) 1992

Chapter 5

LATTICE INSTABILITIES IN NEMATICS AND CHOLESTERICS IN A LASER FIELD

Design's miraculous potency was caught
Laden with beauty and significance..
Sri Aurobindo in Savitri, -p 267

5.1 Introduction

A periodic lattice is formed in a nematic in the presence of an external static field as discussed in the introduction. This is due to the flexoelectric effect. In the presence of another external field this structure becomes a soliton lattice. In a cholesteric an external magnetic or electric field can lead to director reorientation and a uniformly twisted cholesteric becomes a soliton lattice. In this chapter we discuss a few nonlinear optical effects in such soliton lattices due to the director reorientation process. We study the unwinding of the twisted structure in the presence of a laser field and contrast with the same transition which is well studied in the static electric and magnetic fields.

5.2 Nematic in Electric and Optical Fields

In this section we first look at the existence of a flexoelectric lattice in the presence of a combined action of static electric and optical fields. Next, we study the same lattice in the Bragg mode. Finally, we study the implications of Kerr nonlinearity.

5.2.1 Induced flexoelectric lattice

In a nematic made of either pear shaped or banana shaped molecules, the average permanent dipole moment of the phase is zero since they can have two opposite orientations with equal probability. Yet, if there are splay and bend distortions the molecules will rearrange themselves and then the average dipole moment is non-zero leading to a spontaneos polarisation as discussed in chapter 1. This phenomenon is akin to *piezoelectricity* of crystals. It is well known that a static electric field in small dielectric anisotropy materials can lead to an instability leading to a periodic structure. The flexoelectric contribution to the free-energy density is proportional to the strength of the distortion and is linear in the electric field as discussed in the introduction.

The total free-energy density of a nematic in the presence of a static electric field is given by [1]:

$$\mathcal{F} = \frac{K}{2}\left[(\nabla \,.\, \mathbf{n})^2 + (\nabla \times \mathbf{n})^2\right] - eE_s\frac{\partial \phi}{\partial z} + |\epsilon_a^s|E_s^2\cos^2\phi/8\pi \qquad (5.1)$$

where $\mathbf{n}$ is the director, ϕ is the angle made by the director with the z-axis, K is the Frank elastic constant, e is the flexoelectric constant, E_s is the static electric field and $\epsilon_a^s = \epsilon_{\|}^s - \epsilon_{\perp}^s$, the static dielectric anisotropy. If ϵ_a^s and e are of opposite signs, then it can be shown [1] that a splay-bend flexoelectric lattice will be induced by the static electric field. It has been shown in chapter 1 that for this to happen the material constants must satisfy the inequality:

$$|\epsilon_a^s| \leq \pi^3 e^2/K \qquad (5.2)$$

It is a one dimensional splay-bend lattice along the z-axis as shown in figure 5.1 (a).

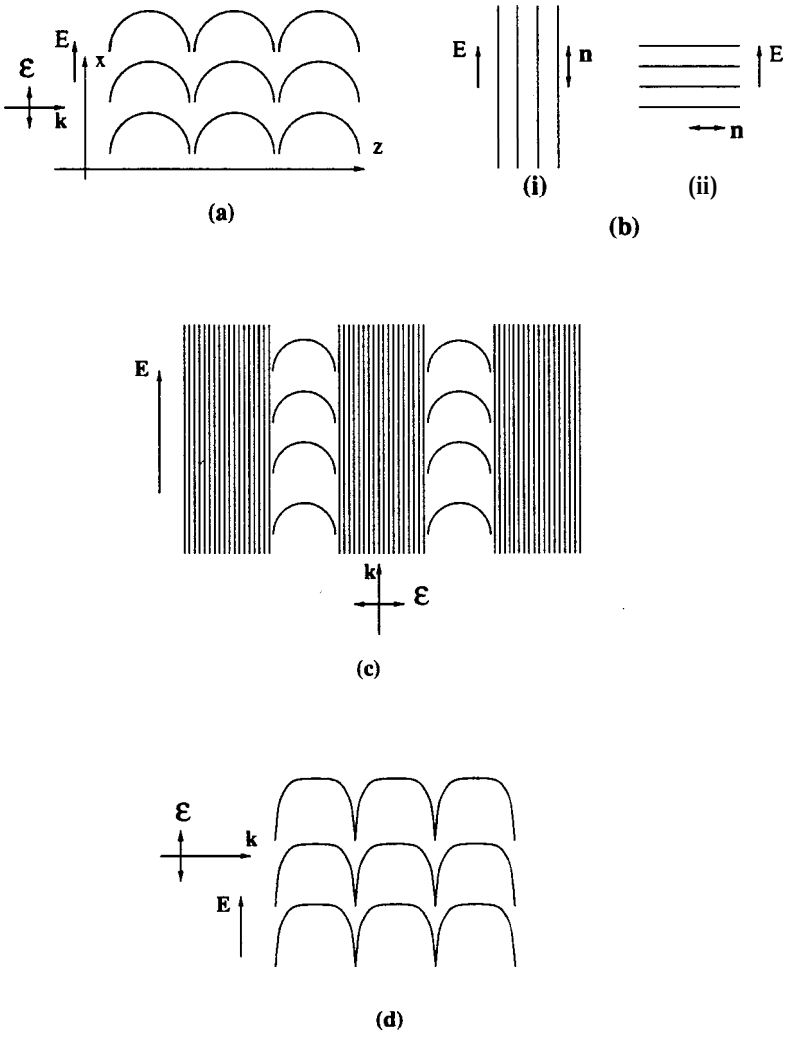

Figure **5.1:** *(a)* **A** *flexoelectric lattice for material parameters which obeys the inequality* **(5.2).** *(b) Uniform state of a nematic (i) along the static electric field@) for* $\epsilon_a^s > 0$ *and (ii) perpendicular to the static electric field for* $\epsilon_a^s < 0$*, for material parameters which does not obey the inequality* **(5.2).** *(c) A j-lexoelectric soliton lattice with the nearly uniform state parallel to E. This structure is obtained if the static dielectric anisotropy is positive and the j-lexoelectric constant is negative. The laser beam is linearly polarized such that its electric vector E is perpendicular to the static electric field E. (d) A j-lexoelectric soliton lattice with the nearly uniform state perpendicular to E. This structure is obtained if the static dielectric anisotropy* is *negative and the j-lexoelectric constant* is *positive. The linearly polarized laser beam has its electric vector E parallel to the static electric field E.*

We consider a nematic with material parameters such that the condition (5.2) is not satisfied. Such nematics do not exhibit a flexoelectric lattice because the dielectric contribution to the free-energy density exceeds that of the flexoelectric contribution. Thus we get a uniform state shown in figure 5.1 (b) with the director parallel(perpendicular) to the static electric field provided ϵ_a^s is positive(negative) and e is negative(positive). The dielectric contribution can be reduced by a linearly polarized laser beam so propagating that its electric vector is perpendicular(parallel) to the static electric field if ϵ_a is positive(negative). This leads to an additional term $(-\epsilon_a^o \mathbf{I} \cos^2 \phi/8\pi c)$, to the free-energy density. Here, ϵ_a^o is the optical dielectric anisotropy. Then we get a flexoelectric lattice above a threshold laser intensity. In the presence of the laser beam the inequality for the absence of the flexoelectric lattice is:

$$\left[|\epsilon_a^s|\, E_s^2/8\pi - \epsilon_a^o\, I/16\pi c\right] \geq \pi^2\, e^2\, E_s^2/8K \qquad (5.3)$$

Thus at high enough intensity we can change the sign of the inequality. This happens above a threshold intensity given by:

$$I_{th}/c = 2(|\epsilon_a^s| - \frac{\pi^3 e^2}{K}) E_s^2/\epsilon_a^o \qquad (5.4)$$

Interestingly, this lattice is not the familiar uniform splay-bend lattice(shown in figure 5.1 (a) but a non-uniform splay-bend soliton lattice with director distortion as shown in figure 5.1 (c) or (d) for two different directions of propagation of the incident laser field, parallel and perpendicular to the direction of periodicity. It has wide regions of uniform alignment.

The evolution of the structure as the laser intensity is increased depends on the geometry. We use a wavelength small compared to the optical period of the structure. The period of the structure increases with the increasing intensity. When the wavelength is greater than the pitch then the pitch increases initially and finally a stage is reached-at which the wavelength of the laser beam matches the period of the flexoelectric lattice leading to diffraction in the case shown in figure 5.1 (c) or Bragg reflections in the case shown in figure 5.1 (d). In the first case the entire structure is

globally distorted and results in a structure similar to a soliton lattice. In the second case we get a large uniform lattice with a small soliton lattice attached to it.

5.2.2 Self-induced oscillations

In a normal flexoelectric lattice when the wavelength of the incident light matches with the optical period we get a standing wave. The amplitude is quite high at the antinodes to lead to a non-uniform distortion at the antinodes. This results in a phase mismatch of the forward and backward propagating waves. The mismatching causes the amplitude at the antinodes to decrease and the structure relaxes back to the original field free state. This allowés for a good phase-matching again and the process continues indefinitely. Hence we expect here the periodic oscillations in the transmitted intensity associated with the structural oscillations.

5.2.3 Effect of Kerr nonlinearity

Liquid crystals like any other medium also possess the familiar classical Kerr nonlinearity. This becomes obvious if we go to geometries where the process of director reorientation is absent. This happens whenever the electric field of a linearly polarized laser beam is parallel(perpendicular) to the director in a $\epsilon_a > 0 (\epsilon_a < 0)$ material. The induced electric polarization in terms of the laser electric field is given by [2]:

$$P_i = \chi_{ij}\mathcal{E}_j + \chi_{ijk}\mathcal{E}_j\mathcal{E}_k + \chi_{ijkl}\mathcal{E}_j\mathcal{E}_k\mathcal{E}_l + ... \tag{5.5}$$

In centro-symmetric materials all odd rank tensors vanishes. Thus χ_{ijk} is zero identically for all achiral systems. Thus we consider only the fourth rank tensor χ_{ijkl} which describes the classical Kerr nonlinearity.

To ascertain the effect of the Kerr nonlinearity we consider the non-vanishing components of the fourth rank tensor χ_{ijkl} for a nematic which is a cylindrically symmetric uniaxial system. This tensor is given by [3]:

$$\begin{pmatrix} \text{xxxxx} & \chi_{yyxx} & \chi_{zzxx} & 0 & 0 & 0 \\ \chi_{xxyy} & \chi_{yyyy} & \chi_{zzyy} & 0 & 0 & 0 \\ \chi_{xxzz} & \chi_{yyzz} & \chi_{zzzz} & 0 & 0 & 0 \\ 0 & 0 & 0 & \chi_{yzyz} & 0 & 0 \\ 0 & 0 & 0 & 0 & \chi_{xzxz} & 0 \\ 0 & 0 & 0 & 0 & 0 & \chi_{xyxy} \end{pmatrix}$$

We saw that for the propagation direction perpendicular to the direction of the periodicity of a flexoelectric lattice and with its electric vector parallel to the periodicity axis we get a soliton lattice. In this geometry the Kerr nonlinearity due to this intense laser beam alone alters the component of the dielectric tensor along the y-axis (the periodicity being along z-axis). Its variation is given by:

$$\begin{aligned} \epsilon'_{yy} &= \epsilon_\perp + \chi_{yyxx}\mathcal{E}_x^2 + \chi_{yyzz}\mathcal{E}_z^2 \\ &= \epsilon_\perp + \mathcal{E}^2(\chi_{yyxx}\cos^2\phi(z) + \chi_{yyzz}\sin^2\phi(z)) \end{aligned} \tag{5.6}$$

Since the director periodically varies with z we find a periodic variation in this component of the dielectric tensor i.e., for a electric vector parallel to the y-axis. The amplitude of the variation is directly proportional to the intensity of the laser beam. It is easy to see that a flexoelectric lattice is optically homogeneous for light incident normal to the x-axis and polarized parallel to it (y-axis) as shown in figure **5.2** (a) for beam **1.** Interestingly, this will not be true if the Kerr effect is included. The structure which is normally homogeneous for a weak light beam **1** becomes optically periodically inhomogeneous in the presence of the strong laser beam **2** propagating in the same direction but polarized in an orthogonal direction (z-axis). Thus we get a new diffraction mode in a flexoelectric lattice(cf. figure **5.2** (b)). The peculiarity of this geometry is that the intense laser beam leads to a soliton lattice due to the accompanying director reorientation. At high enough intensities the period of the structure becomes so large that the new diffraction pattern shrinks considerably. This can be circumvented if a static magnetic field is applied along the x-axis. The free-energy density is:

$$\mathcal{F} = \mathcal{F}_\circ + K\left(\frac{\partial\phi}{\partial z}\right)^2 - \frac{\chi_a \mathbf{H}^2}{2}\cos^2\phi - \frac{\epsilon_a I}{16\pi c}\sin^2\phi - eE\frac{\partial\phi}{\partial z} \tag{5.7}$$

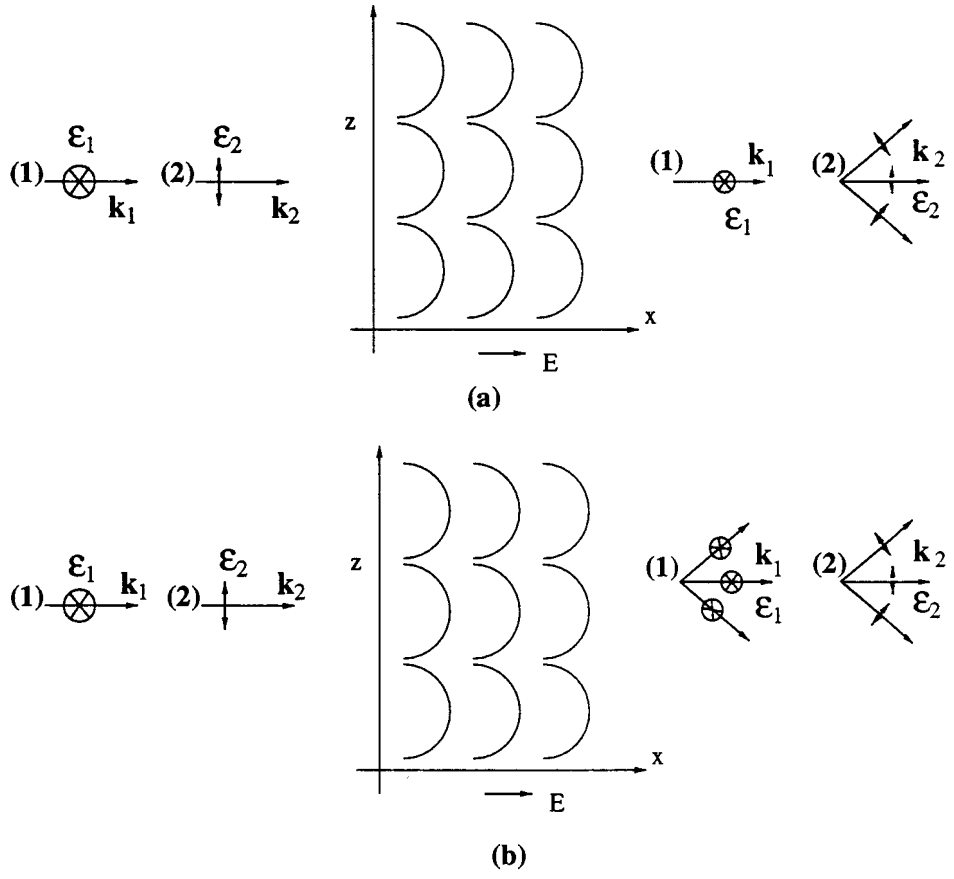

Figure **5.2:** *The diffraction mode in a flexoelectric lattice. (a) The electric vector of the weak beam (beam 1) is along the y-axis. This passes through the medium without undergoing any diffraction. A laser beam (beam 2) is propagating in the same direction but polarized along the z-axis. (b) At higher intensities even the beam 1 suffers diffraction due to the Kerr effect induced by beam 2.*

At a magnetic field strength $H = \sqrt{\frac{\epsilon_a I}{c \chi_a}}$ (which increases with laser intensity). we get a uniform lattice. Thus the effect due to Kerr nonlinearity alone can be enhanced by increasing the laser intensity with a corresponding increase in H.

5.3 Cholesteric in the Bragg Mode

We consider light propagation along the twist axis in the three limits viz..

(a) $\lambda \ll \Delta\mu P$ i.e., the short wavelength limit or the *Mauguin limit* (figure **5.3** *(a)* and (b)),

(b) $\lambda \sim \mu P$ i.e., for wavelengths inside the *Bragg band* and

(c) $\Delta\mu P < \lambda < \mu P$ and $\lambda \gg \mu P$ or the *de Vries* limits.

Here ***P*** is the pitch, $\Delta\mu$ is the local birefringence and μ is the average refractive index.

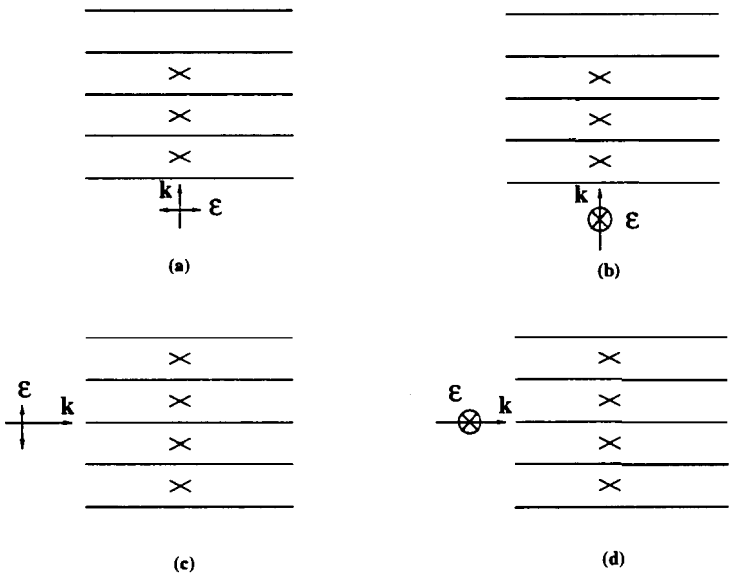

Figure 5.3: *(a) The laser beam is propagating parallel to the twist axis of a cholesteric and the electric vector is parallel to the director everywhere. (b) The laser beam is propagating parallel to the twist* axis *of a cholesteric and the electric vector is perpendicular to the director everywhere. (c) The laser beam is propagating perpendicular to the twist axis and the electric vector is parallel to the twist axis. (d) The propagation direction is perpendicular to the twist axis with the electric vector also perpendicular to the twist axis. Full line indicates the director in the plane of the paper and* $\times$ *indicates that it is perpendicular to the plane of the paper.* $\mathcal{E}$ *is the electric field and k the direction of propagation of the laser beam.*

5.3.1 Self-induced oscillations

It is useful to recall here that for a circular polarisation which has the same sense as the helix of the cholesterics, they reflect totally all wavelengths within the Bragg band of wavelengths of width AX $= \Delta\mu P$ centered around $\lambda_\circ = \mu P$ [4]. This reflected circular wave interferes with the forward propagating circular wave and sets up a standing wave inside the medium which is linearly polarized. At the long wavelength edge of the Bragg band its electric vector is parallel to the local director while it is perpendicular to the local director at the short wavelength edge of the reflection band. Inside the Bragg band the linearly polarized standing wave has its electric field at an angle to the local director [5] and its intensity exponentially decreases with distance from the boundary on which the circularly polarized beam is incident. Inside the Bragg band of wavelengths at higher laser intensities the dielectric torque on the director due to the electric field of a standing wave reorients the director. As the electric field inside

the medium is non-uniform the resulting torque and hence the induced local twist is also non-uniform. Just as in the case discussed earlier for flexoelectric lattice: a strict phase-matching between the waves reflected from different regions of the periodic structure is not possible. In such a situation we again find ***self – induced oscillations*** in the reflected and transmitted intensities accompanied with local oscillations in the twist. The time scale involved in this process is the time required for the director to relax which is of the order of $\eta/K_{22}q^2$, η being the twist viscosity constant, K_{22}, the twist elastic constant and q, the wavevector of twist distortion. This relaxation time is in the range of milliseconds to seconds. Correspondingly, the frequency of the oscillations is typically between a few kHz to one Hz. This effect will be a maximum at the short wavelength edge of the reflection band at which the net electric vector is perpendicular to the local director. At the long wavelength edge the same effect will be absent since here the net electric vector is along the local director. Similar effects are found even in the case of negative dielectric anisotropic materials. In this case the effect is maximum at the long wavelength edge of the Bragg band while it is absent at the short wavelength edge.

5.3.2 Unwinding of the helix- long wavelength limit

We consider next cholesterics at wavelengths(λ) greater than μP. In this case: as is well known [4], the system exhibits a weak optical rotation. This rotation falls as $1/X^2$ [6]. Since the wavelength is very large compared to the pitch we can ignore this weak optical rotation. Then it is equivalent to a cholesteric in a static electric or magnetic field acting perpendicular to the twist axis. This problem has been studied by de Gennes [7] and Meyer [8] and was discussed in detail in Chapter 1. The field induces a soliton lattice whose period increases with the field strength and finally becomes infinity at a critical field strength (see figure 1.10). We expect a very similar result in an intense laser beam. However, in the presence of a laser beam as the pitch increases it eventually leads to a pitch that satisfies the Bragg condition and hence to a total reflection of the incident light. In the region where the light beam does

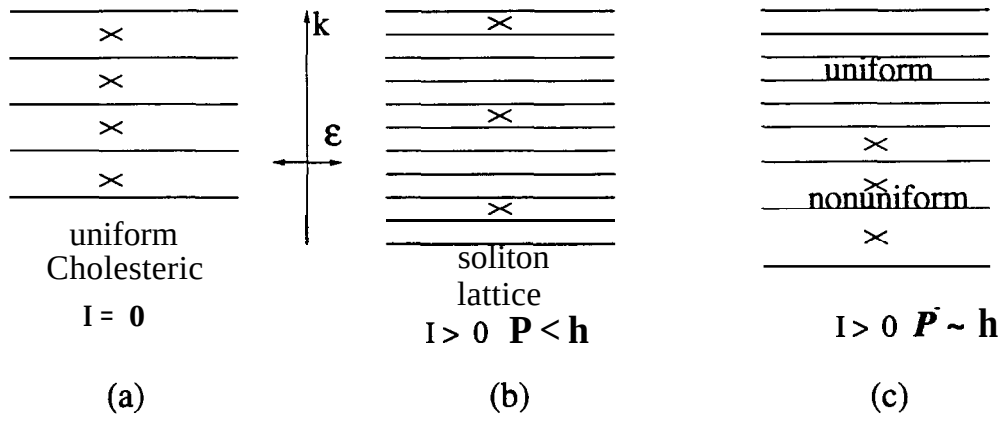

Figure 5.4: *The figure depicts a non-uniform cholesteric appended to almost uniform cholesteric which results when the laser beam is propagating in the Bragg mode.*

not enter we get a uniform cholesteric. Hence, we end up with a uniform cholesteric appended by a small region that is reflecting the incident light as shown in figure 5.4. When $\Delta\mu P < \lambda < \mu P$ we get a high optical rotation. Hence, the problem of director reorientation along with the changes in optics is hard to analyze. Only a numerical approach is possible. Thus we see that a cholesteric to nematic transition in the presence of a laser field is entirely different from that taking place in a static field. The same effects are to be expected in the case of materials with negative dielectric anisotropy. As chiral smectic C is also a twisted structure, an analogous behavior is to be found in these systems. In chiral smectic C the c-director in the plane of the layers is similar to the nematic director and the unwinding transition here implies that the c- director in all layers are aligned parallel to each other. This configuration is similar to the smectic C phase where the molecules are all tilted in the same plane.

5.4 Cholesteric in the Diffraction Mode

In this case we consider seperately the two situations namely, $\lambda \ll \mu P$ and $\lambda \gg \mu P$.

5.4.1 Short wavelength limit: $\lambda \ll \mu P$

We assume that the laser beam propagates with its electric vector perpendicular to the helix axis. Excepting at some regularly spaced points elsewhere, the electric vector will be at an angle to the director. This angle periodically varies as we go

along the twist axis(see figure 5.3 (d)). Again free-energy is same as earlier and we get as in the previous case a soliton lattice due to the laser reorienring torque acting on the director. In this case the refractive index of the medium periodically varies for this polarization. Thus an incident plane wavefront emerges as a corrugated wavefront. This leads to a phase grating effect resulting in optical diffraction. In thin samples internal optical diffraction would be negligible and we get a transition to the completely unwound state at a critical intensity, given by:

$$I_c = (16\pi^5 cK/\epsilon_a)\frac{1}{P_\circ}$$

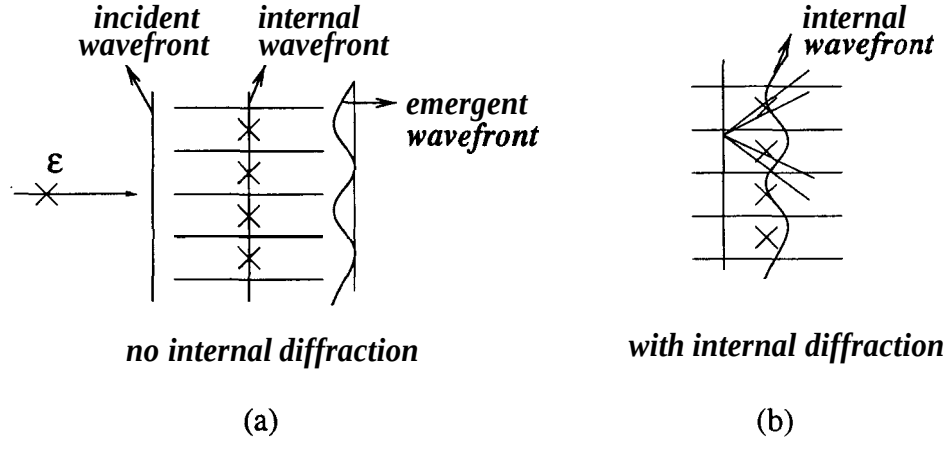

Figure 5.5: *Diffraction mode. (a) In thin samples the laser beam does not undergo much diffraction (b) In the case of thick samples diffraction cannot be neglected.*

However, in thick samples internal diffraction cannot be ignored and the laser intensity gets distributed amongst the various orders of diffraction inside the medium as shown in the figure 5.5. This stabilizes the structure in a periodically distorted state preventing the laser field from completely unwinding the chiral stare.

5.4.2 Long wavelength limit: $\mu P \ll \lambda$

The incident laser beam again has its electric vector perpendicular to the helix axis. In this limit the laser field simulates more or less the effect of a static field case. The helix gradually starts unwinding. As the pitch increases and becomes comparable to the wavelength, diffraction takes over. Again it is not difficult to see that the chiral-achiral transition is possible only in thin samples.

5.5 Reorientation of the Twist Axis

Consider an unbounded i.e., a free cholesteric liquid crystal. Now we ask ourselves the question of what would happen if a linearly polarized laser beam falls on the structure. We study three special cases.

(i) $\lambda \ll \Delta\mu P$: This happens typically for wavelengths less than $(1/10)^{th}$ of the pitch of the cholesteric. If the structure adopts a configuration with the twist

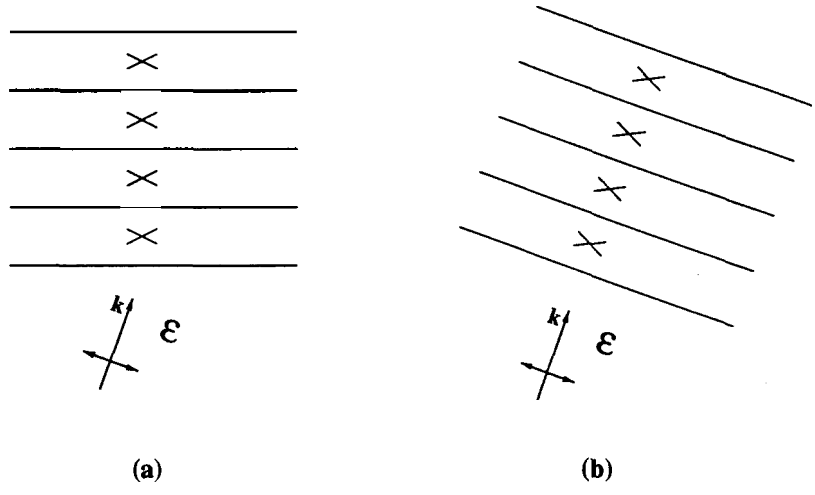

Figure 5.6: *The figure (a) depicts a cholesteric at low incident laser intensity and (b) shows the reorientation of the twist axis when the intensity of the laser is increased.*

axis along the direction of the laser beam, then the system is optically in the short wavelength or Mauguin limit. If the electric field of the laser beam is parallel to the local director then there is no torque acting on the director when the dielectric anisotropy is positive. The structure is then identical to the field free twisted state (see figure 5.6). Therefore, this state is preferred by the system. In case of materials with negative dielectric anisotropy in both the geometries viz., **(i)** twist axis parallel to the direction of propagation it is in the Mauguin limit with the electric vector perpendicular to the local director everywhere (see figure *5.3 (b))* and (ii) twist axis perpendicular to the direction of propagation with the electric vector parallel to the twist axis, the structure is undistorted (see figure *5.3 (c))*. Hence, a degeneracy in the helix axis orientation exists for $\Delta\mu < 0$ cholesterics.

(ii) $\lambda \sim \mu P$. In this case there is Bragg reflection, for twist axis parallel to the

direction of propagation and diffraction for twist axis perpendicular to the direction of propagation. In the first case the structure is mostly undistorted excepting near the boundary on which the laser is falling. Hence, within a penetration depth it suffers non-uniform distortion. In the second case there is a global distortion leading to a soliton lattice which has a higher elastic distortion energy. Therefore we expect the helix axis to be aligned along the direction of propagation i.e., the situation shown in figure 5.4.

(iii) $\lambda \gg \mu P$. In this case, as already said the laser field simulates the case of a static field leading to a soliton lattice. With increase in intensity, the pitch increases. When the condition $\mu P \approx \lambda$ is satisfied we get either Bragg reflection or the diffraction of light resulting in a nonuniformly twisted structure. However, distortion is confined to a small region in the Bragg mode. Hence this will be the preferred state at high intensities. The configuration is again as shown in figure 5.4.

5.6 Effect of Classical Optical Kerr Nonlinearity

To ascertain the effect of the Kerr nonlinearity in cholesterics we note that the cholesterics can be looked upon locally as nematics. Thus locally the symmetry of the cholesteric is same as the nematic and thus the Kerr nonlinearity is again described by the same fourth rank tensor as discussed under nematics.

We saw that for the propagation direction perpendicular to the twist axis with its electric vector also perpendicular to the twist axis we get a soliton lattice. In this geometry Kerr nonlinearity due to this intense laser beam alone alters the component of the dielectric tensor along the twist axis (y-axis). Its variation as in the case of a flexoelectric lattice is given by:

$$\begin{aligned} \epsilon'_{yy} &= \epsilon_\perp + \chi_{yyxx}\mathcal{E}_x^2 + \chi_{yyzz}\mathcal{E}_z^2 \\ &= \epsilon_\perp + \mathcal{E}^2(\chi_{yyxx}\cos^2\phi(y) + \chi_{yyzz}\sin^2\phi(y)) \end{aligned} \tag{5.8}$$

Since ϕ periodically varies with y we find a periodic variation in this com-

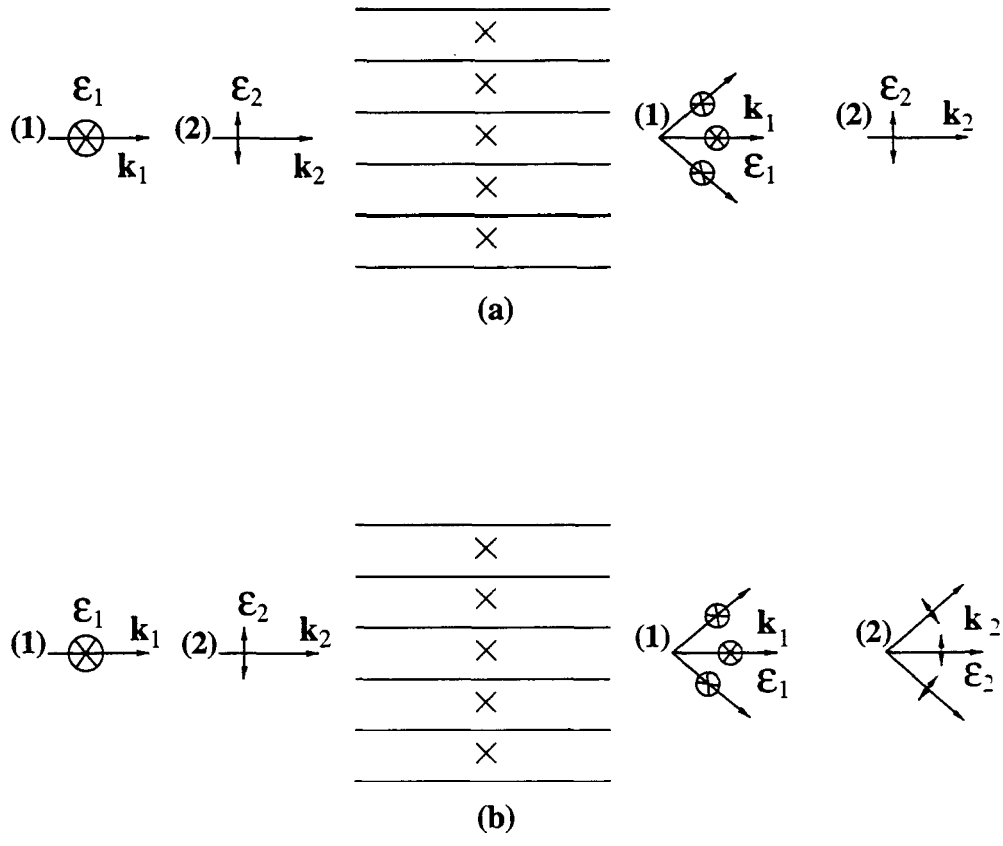

Figure 5.7: *The diflraction mode in a cholesteric. (a) The electric vector of the laser beam 1 is perpendicular to the twist axis. This always undergoes diffraction. A weak beam 2 is propagating in the same direction but polarized parallel to the twist axis. At low intensities of beam 1, we find that beam 2 is not diffracted. (b) At higher intensities of the beam 1, the same beam (beam 2) suffers diffraction.*

ponent of the dielectric tensor i.e., for a electric vector parallel to the twist axis. The amplitude of the variation is directly proportional to the intensity of the laser beam. As already said a cholesteric is normally optically homogeneous for light incident normal to the twist axis and polarized parallel to it as shown in figure 5.7 (a). The structure which is normally homogeneous for a weak light beam now becomes optically periodically inhomogeneous in the presence of the strong laser beam propagating in the same direction but polarized in an orthogonal direction. Thus we get a new diffraction mode in a cholesteric(cf. figure 5.7 (b)). The peculiarity of this geometry is that the intense laser beam leads to a soliton lattice due to the accompanying director reorientation. At high enough intensities the period of the structure becomes so large that the new diffraction pattern shrinks considerably. As discussed

earlier in the case of flexoelectric lattices, the effect of director reorientation can be circumvented if a static magnetic field is applied perpendicular to the twist axis and the electric field of the laser. At a magnetic field strength $H = \sqrt{\epsilon_a I/c\chi_a}$ (which increases with laser intensity), we get a uniformly twisted state. This enables us to consider the effect due to Kerr nonlinearity alone.

5.7 Instability in Confined Geometries

As said in the introductory chapter, in the coarse-grained approximation [4, 6], a cholesteric behaves like a smectic *A*. It can be treated as though it is made of layers with each layer having a thickness equal to half the pitch. In a confined geometry with twist axis perpendicular to the plates, with a magnetic field acting along the twist axis we get an undulation instability. The undulation instability occurs due to the competition between the diamagnetic energy and the anchoring energy at the boundaries. The layers undergo a periodic distortion perpendicular to the field. The relevant free-energy density is given by:

$$\mathcal{F} - \mathcal{F}_o = \frac{B}{2}\left(\frac{\partial u}{\partial z}\right)^2 + \frac{K'}{2}\left(\frac{\partial^2 u}{\partial x^2} + \frac{\partial^2 u}{\partial y^2}\right)^2 - \chi_a H^2 \left(\frac{\partial u}{\partial x}\right)^2 \tag{5.9}$$

Here $B = K_2 q_o^2$ with q_o being the wavevector of inherent cholesteric twist periodicity, is the effective elastic constant for lattice stretching or compression. $K' = 3K/8$ is an effective curvature elastic constant. The critical field at which this instability is induced is given by:

$$H_c = 2\pi \frac{B\alpha}{d} \tag{5.10}$$

and the wavevector of the periodicity is then given by:

$$k^2 = \pi/\alpha d \tag{5.11}$$

where $a = \sqrt{K'/B}$. In experiments this instability is observed as a square lattice which is a superposition of the two periodic distortions oriented at right angles. We discuss this instability here in the presence of a laser beam with optical dielectric anisotropy being either positive or negative.

It has been said already that a cholesteric liquid crystal behaves optically as a homogeneous medium for a laser beam propagating perpendicular to its twist axis and with its electric vector parallel to the twist axis (figure 5.3 (c)). The sample thickness *(d)* should be much larger than the wavelength of the laser beam. Otherwise there will be *'slit'* diffraction due to finite sample thickness on entering into the sample. In an anchored finite sample with positive dielectric anisotropy this can lead to an undulation instability just as in static fields [4]. The threshold intensity for the instability to set in can be easily obtained from a simple generalisation of the equation (5.9). It is given by:

$$\frac{I_{th}}{c} = \frac{16\,\pi^2\,K}{\epsilon_a\,\alpha\,d} \tag{5.12}$$

The ensuing distortion is schematically shown in figure 5.8 (b).

Assuming, $\epsilon_a = 0.1$, $\mathbf{K} = 10^{-11}$ *newton*, $\mathrm{P} = 20$ *pm*, d = 100 pm we get the

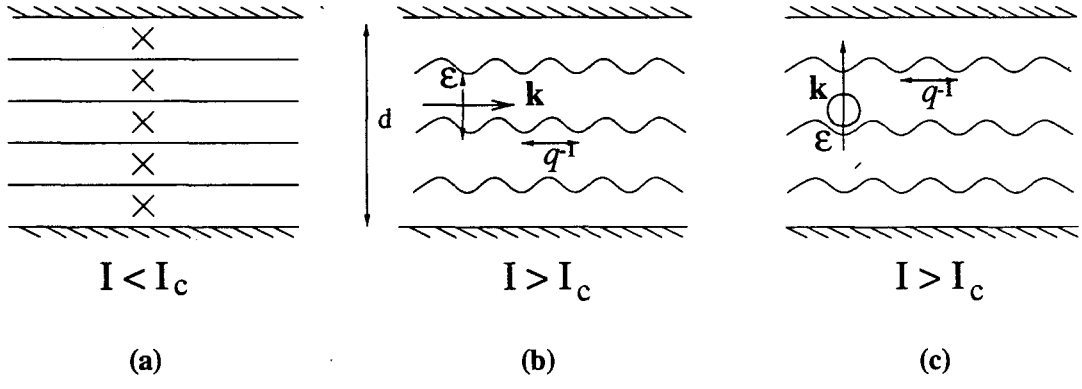

Figure 5.8: *The distortion of a cholesteric in an undulation instability. d is the sample thickness. (b) Here $\epsilon_a > 0$ and the sample thickness is very large compared to the wavelength. Incident laser beam is linearly polarized perpendicular to the plates and propagating parallel to the plates. The wavevector q of this distortion is along the direction of propagation of the laser beam. (c) Here $\epsilon_a < 0$. Incident light is circularly polarized in a sense opposite to that of a cholesteric and is propagating perpendicular to the plates. In this case the wavevector of distortion is across the wavefront of the incident laser beam.*

threshold intensity to be $3 \cdot 10^4\ kW/m^2 (3\ kW/cm^2)$, which is easily realizable. If the local dielectric anisotropy is negative then we send the laser beam along the twist axis. If the structure is not in the Mauguin limit then the eigen modes in this case are right and left circular polarized waves. In order to avoid Bragg reflection we

illuminate the sample with a circularly polarized light whose sense is opposite to the sense of the cholesteric. Again layer undulation instability sets in beyond a threshold intensity which is the same as that given by equation (5.12). It is easy to see that in this case the periodic distortion as shown in the figure 5.8 (c) is across the plane wavefront of the incident beam. When the wavelength of the light is small compared to the wavelength of the distortion, the laser beam gets diffracted. If the sample thickness is so small that the internal diffraction can be ignored. then the evolution of structural distortion with increase of intensity will be rather close to that found in the static fields. In the case of thick samples, internal diffraction becomes important. Then just above the threshold, light gets redistributed between the different orders of diffraction leading to a different periodic structure. In cases where the wavelength of light, λ is much greater than q^{-1} then there will be no diffraction and we just get the same result as that found in static fields.

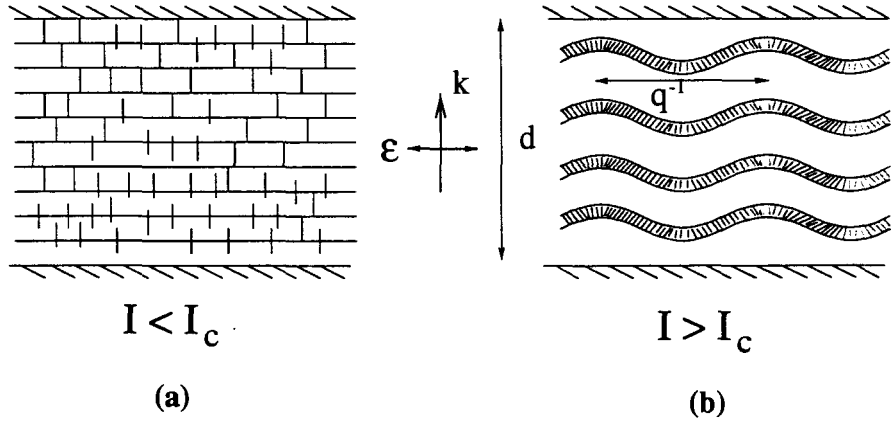

Figure 5.9: *The distortion of a smectic due to laser induced undulation instability. d is the sample thickness. (b) Here $\epsilon_a > 0$ and the sample thickness ti very large compared to the wavelength. Incident laser beam is linearly polarized parallel to the plates and propagating perpendicular to the plates. The wavevector q of this distortion is perpendicular to the dzrection of propagation of the laser beam which leads to diffraction. If $\epsilon_a < 0$ we send light parallel to the plates with $\mathcal{E}$ along the layer normal. Again we get an identical instability.*

The same instability can also be observed in smectic A with positive dielectric anisotropy in a homeotropically aligned sample. Here a linearly polarized laser beam propagating along the layer normal as shown in figure 5.9 induces the

instability. The laser beam is diffracted if the wavelength of light is less than the induced periodicity. In materials with negative dielectric anisotropy, the laser beam propagating along the layers with its electric vector parallel to the layer normal leads to the same instability. The threshold intensity for the onset of instability is again given by equation (5.12). For typical values of the smectic material parameters and $d = 300\ \mu m$, the threshold intensity is $\approx 25 \cdot 10^4$ kW/m^2(25 kW/cm^2) which again is also presently attainable. Incidentally, for the same sample thickness, to induce the same instability we require a magnetic field as high as 120 kG [6].

Bibliography

[1] S. A. Pikin, *Structural Transformations in Liquid Crystals* (Gordon and Breach Science Publishers, New York), 1991

[2] Y. R. Shen, *The Principles of Nonlinear Optics* (John Wiley and sons, New York) 1984

[3] J. F. Nye, *Physical Properties of Crystals* (Oxford University Press, London) 1957

[4] S. Chandrashekar, *Liquid Crystals* (second edition), Cambridge University Press, Cambridge) 1992

[5] R. Nityananda et. al., Pramana, *Suppl.No1*, 325-340 (1975)

[6] P. G. de Gennes and J. Prost. *The Physics of Liquid Crystals* (Oxford Science Publications, Oxford) 1993

[7] P. G. de Gennes, Solid State Commun., 6, 163 (1968)

[8] R. B. Meyer, **App.** Phy. Lett.. **14,** 208 (1969)